



# DIGITAL ACCESS TO SCHOLARSHIP AT HARVARD

## Single-File Diffusion of Flagellin in Flagellar Filaments

The Harvard community has made this article openly available.  
[Please share](#) how this access benefits you. Your story matters.

<b>Citation</b>	Stern, Alan S., and Howard C. Berg. 2013. Single-File Diffusion of Flagellin in Flagellar Filaments. <i>Biophysical Journal</i> 105, no. 1: 182–184.
<b>Published Version</b>	<a href="https://doi.org/10.1016/j.bpj.2013.05.030">doi:10.1016/j.bpj.2013.05.030</a>
<b>Accessed</b>	February 19, 2015 5:13:42 PM EST
<b>Citable Link</b>	<a href="http://nrs.harvard.edu/urn-3:HUL.InstRepos:12336269">http://nrs.harvard.edu/urn-3:HUL.InstRepos:12336269</a>
<b>Terms of Use</b>	This article was downloaded from Harvard University's DASH repository, and is made available under the terms and conditions applicable to Other Posted Material, as set forth at <a href="http://nrs.harvard.edu/urn-3:HUL.InstRepos:dash.current.terms-of-use#LAA">http://nrs.harvard.edu/urn-3:HUL.InstRepos:dash.current.terms-of-use#LAA</a>

*(Article begins on next page)*

## Single-File Diffusion of Flagellin in Flagellar Filaments

Alan S. Stern<sup>†</sup> and Howard C. Berg<sup>†\*</sup>

<sup>†</sup>Rowland Institute at Harvard and <sup>‡</sup>Department of Molecular and Cellular Biology, Harvard University, Cambridge, Massachusetts

**ABSTRACT** A bacterial flagellar filament is a cylindrical crystal of a protein known as flagellin. Flagellin subunits travel from the cytoplasm through a 2 nm axial pore and polymerize at the filament's distal end. They are supplied by a pump in the cell membrane powered by a proton-motive force. In a recent experiment, it was observed that growth proceeded at a rate of approximately one subunit every 2 s. Here, we asked whether transport of subunits through the pore at this rate could be effected by single-file diffusion, which we simulated by a random walk on a one-dimensional lattice. Assuming that the subunits are  $\alpha$ -helical, the answer is yes, by a comfortable margin.

### INTRODUCTION

The external structures of a bacterial flagellum include a proximal hook (FlgE), which acts as a universal joint; two hook-associated proteins (FlgK and FlgL), which mate the flexible hook to the rigid helical filament (FlgC); and another hook-associated protein (FlgD), which serves as a cap (1,2). Flagellin is secreted into the filament at its base via the proximal hook and two hook-associated proteins by a transmembrane pump driven by a proton-motive force (3,4). Subunits of FlgC travel along the axis of the filament through a pore ~2 nm in diameter (5) and crystallize at the distal end. Crystallization is orchestrated by a FlgD pentamer (6). If FlgD is missing, flagellin is simply dumped out into the external medium (7). The hook-associated proteins can be found in the external medium, suggesting that caps that are lost when filaments break can be replaced (8).

In recent work, we confirmed that broken filaments continue to grow (9). Cells were grown for ~4 h and their filaments (containing cysteine) were stained with a sulfhydryl-specific green fluorescent dye. The filaments were then sheared or not, the cells were grown for an additional 4 h, and the filaments were stained again with a sulfhydryl-specific red fluorescent dye. Comparisons of the distributions of lengths of green, red, or green + red segments enabled us to conclude that the sheared filaments continued to grow. However, we also found for the unsheared populations that the lengths of red segments did not depend on the lengths of green segments from which they grew. We suggested that the pump at the base of the flagellum injects flagellin into the filament pore at a constant rate, approximately one subunit every 2 s. The longest filament recorded in these experiments was 13  $\mu\text{m}$ .

For this model to work, subunits must reach the distal end of the pore at approximately the same rate at which they are pumped in. They have to move through the pore in single file, without passing any other subunits. Here, we simulated

this process by allowing subunits to execute a random walk on a one-dimensional lattice.

In this work, our interest is in filament growth, not in the physics of single-file diffusion. For a taste of the latter subject, see Lutz et al. (10).

### RESULTS AND DISCUSSION

We assume that the subunits move as extended  $\alpha$ -helical chains, ~1 nm in diameter by 74 nm long (9), along a lattice with spacing equal to the subunit length, as shown in the scale drawing of Fig. 1. We choose a step interval equal to the time it takes such a subunit to diffuse a distance equal to its length. The frictional drag coefficient,  $f_1$ , for a prolate ellipsoid of half-length  $a = 37$  nm and radius  $b = 0.5$  nm moving along its long axis in a medium of viscosity  $\eta$  is  $f_1 = 4\pi\eta a / [\ln(2a/b) - 1/2]$ , which for  $\eta = 0.7 \times 10^{-3}$  kg/sm (water at 30°C) is  $7.24 \times 10^{-11}$  kg/s (see Fig. 4.5 in Berg (11)). The diffusion coefficient at  $T = 303$  K is  $D = k_B T / f_1 = 5.78 \times 10^{-11}$  m<sup>2</sup>/s. The step interval for this diffusion coefficient is  $\tau = (2a)^2 / 2D = 4.7 \times 10^{-5}$  s. Below, we will deal with the fact that the actual diffusion coefficient for movement in a 2 nm pore must be substantially smaller than this initial estimate. One subunit extending 74 nm in the pore is surrounded by 156 subunits in the filament (9,12), so once 156 subunits have passed through the pore and crystallized out at the distal end, we extend the lattice by one site.

Assume that the pore extends from the base at the left to the tip at the right. For each time step (one step interval), the simulation program looks at the subunits one at a time, alternating right-to-left and left-to-right in successive time steps. Each subunit moves one site, right or left with probability 1/2, unless the destination site already is occupied, in which case it does not move. The fictitious position to the left of the leftmost site is considered to be always occupied, and the fictitious position to the right of the rightmost site is considered to be always vacant. New subunits attempt to enter the leftmost site at an average rate of one every

Submitted April 17, 2013, and accepted for publication May 20, 2013.

\*Correspondence: hberg@mcb.harvard.edu

Editor: Dennis Bray.

© 2013 by the Biophysical Society  
0006-3495/13/07/0182/3 \$2.00

<http://dx.doi.org/10.1016/j.bpj.2013.05.030>



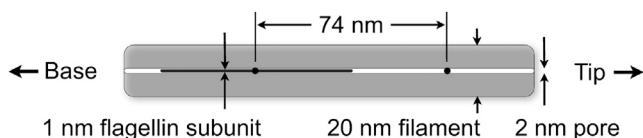


FIGURE 1 Scale drawing of a short segment of a flagellar filament containing one  $\alpha$ -helical flagellin subunit, 1 nm in diameter  $\times$  74 nm long. The subunit executes a random walk along a one-dimensional lattice with spacing equal to the subunit length. Two lattice sites are shown (solid circles). The subunit source is at the base of the filament, far to the left. The subunit sink is at the tip of the filament, far to the right. A filament 7.4  $\mu\text{m}$  long would span 100 lattice sites.

2 s; however, they do not get put on the leftmost site until that site is vacant. If a second subunit attempts to enter while the first is still waiting, the second one is blocked; it diffuses away and is lost. Subunits leave the simulation (crystallize out) when they take a rightward step from the rightmost site. We record, as a function of time, the filament length and the fraction of sites that are occupied.

The results for three diffusion coefficients  $\sim 30$ , 120, and 480 times smaller than our initial estimate are shown in Figs. 2 and 3. Fig. 2 shows the filament length as a function of time, and Fig. 3 shows the fraction of sites occupied as a function of time. For the largest diffusion coefficient, both the filament length and the fraction of occupied sites increase linearly. For the smaller diffusion coefficients, the growth rate begins to decline and the occupancy approaches 0.5.

The growth will remain linear as long as the occupancy of the leftmost site is low enough to allow new subunits to enter without blocking further entrants. The average concentration of subunits is expected to decrease from the source at the left to the sink at the right. Beyond site  $N$  at the right, the concentration is zero, and if site 1 at the left

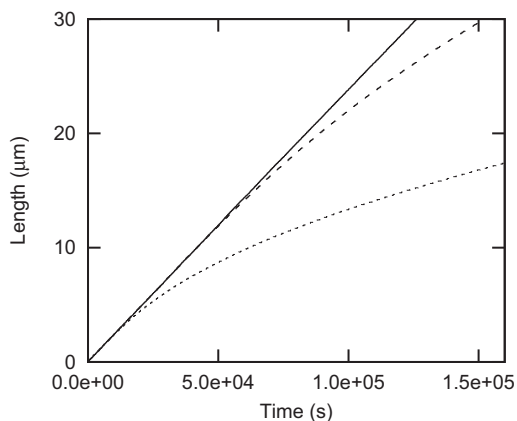


FIGURE 2 Filament lengths shown as a function of time for simulations using diffusion coefficients for flagellin subunits  $D = 2 \times 10^{-12}$  (solid curve),  $5 \times 10^{-13}$  (dashed curve), and  $1.25 \times 10^{-13}$  (dotted curve)  $\text{m}^2/\text{s}$ ,  $\sim 30$ , 120, and 480 times smaller than that estimated for a prolate ellipsoid the size of an  $\alpha$ -helical flagellin subunit diffusing freely in water in the direction of its long axis.

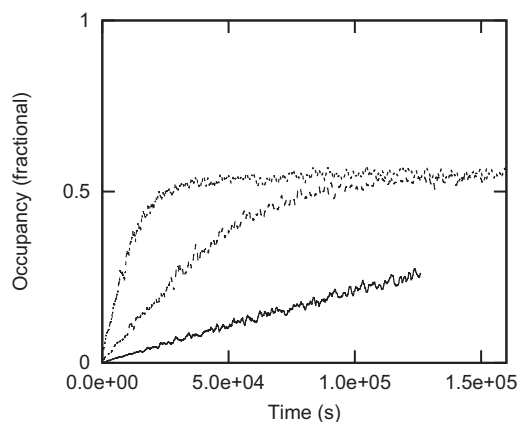


FIGURE 3 Fraction of sites occupied by subunits for the diffusion coefficients used in Fig. 2. When the occupancy is relatively small, the growth rates (indicated by the slopes of the curves in Fig. 2) remain constant. The occupancy was recorded every time a subunit entered or left the filament, and was smoothed by averaging over intervals of 1000 s.

is too crowded for a new subunit to enter quickly, then its average concentration must be close to one. Assuming a linear gradient, the average concentration of site 2 will be  $(N-1)/N$ , which means the site is vacant for only one time step out of every  $N$ . A subunit at site 1 will step right to site 2 with probability  $1/2$ ; hence, a subunit entering site 1 will not leave until  $\sim 2N$  time steps have elapsed. Blockage will thus start to become significant if  $2N\tau$  is larger than the average time between arrival of new subunits, i.e., when  $N = (2 \text{ s})/(2\tau)$ . For the diffusion coefficients used in the figures, this value of  $N$  occurs at lengths of 54, 14, and 3  $\mu\text{m}$ , respectively, which is in good agreement with the curves in Fig. 2.

To obtain a ballpark estimate of how many times smaller the diffusion coefficient for a flagellin subunit might be when moving in a pore of twice its diameter than when moving in an infinite pond, we modeled the subunit as an iron rod and estimated its frictional drag coefficient from the rate at which it fell through a tube filled with a viscous fluid (polydimethylsiloxane, 5000 cSt, specific gravity 0.975; Clearco Products, Bensalem, PA). We chose an aspect ratio for the rod of 1:20 rather than 1:74 to keep the tube of manageable length (for the rod: 1/8 inch diameter ( $3.175 \times 10^{-3}$  m)  $\times$  2 1/2 inches long ( $6.35 \times 10^{-2}$  m), weight  $4.057 \times 10^{-3}$  kg, minus  $4.91 \times 10^{-4}$  kg to correct for buoyancy =  $3.566 \times 10^{-3}$  kg; for the tube: 1/4 inch inside diameter  $\times$  23 inches long). The tube was marked off in 0.1 m intervals, and a stopwatch was started when the bottom of the rod reached 0.1 m and stopped when it reached 0.4 m. Seven trials yielded rates of descent ranging from 1.6 to  $2.0 \times 10^{-3}$  m/s (mean  $\pm$  SD =  $1.77 \pm 0.14$ ). The rate was smaller when the rod slid along the side of the tube, a problem that was mitigated by an occasional tug from a magnet. The Reynolds number was small,  $(6.35 \times 10^{-2} \text{ m}) \times (1.77 \times 10^{-3} \text{ m/s}) / (5 \times 10^{-3} \text{ m}^2/\text{s}) = 2.25 \times 10^{-2}$ .

Applying the formula for the frictional drag coefficient of a prolate ellipsoid to the rod, we get  $f_1 = 0.61 \text{ kg/s}$ . The rate of descent will be  $v = mg/f_1$ , where  $m$  is the mass of the rod corrected for buoyancy, and  $g$  is the acceleration due to gravity ( $9.81 \text{ m/s}^2$ ). Thus,  $v = 5.73 \times 10^{-2} \text{ m/s}$ . This is 32 times larger than the rate of descent measured in the tube, so the diffusion coefficient for the flagellin subunit in the filament pore should be  $\sim 32$  times smaller than our original estimate. So, if it is simply a matter of hydrodynamics, the single-file diffusion model is viable, as shown in Fig. 2. Figs. 2 and 3 include the behavior that is expected if the diffusion coefficient is even smaller, by an additional factor of 4 or 16. A smaller diffusion coefficient is expected if interactions between the subunit and the pore wall impose significant energy barriers that subunits must cross.

As a reality check, we measured the rate of descent of the rod in our polydimethylsiloxane in a graduated cylinder of inside diameter 25.4 times the rod diameter, obtaining a value of  $3.0 \times 10^{-2} \text{ m/s}$ , which reduces the factor of 32 to 1.8. This seems reasonable.

In this model, the pump at the base of the flagellum does not generate a pressure head that drives subunits through the pore (13). Nor does it maintain a constant subunit concentration at the base, with subunits crystallizing at the distal end in a concentration-dependent manner (14). It simply meters subunits into the pore at a specified rate. If another subunit is in the way, it pauses. The same is true for all the subunits in the pore: if other subunits are in the way, they pause. There are no forced movements. If the diffusion coefficient is large enough, the pore is mostly empty, pauses are inconsequential, and the rate of crystallization equals the specified rate of pumping. If the diffusion coefficient is small, the subunits back up until the pore is approximately half full and the rate of pumping declines. We assume that the subunits are partially folded, mainly as  $\alpha$ -helices, which is the conformation at the N- and C-termini of flagellin in the crystal state (5). Unlike earlier proposals, based upon the belief that filament growth rates decline at a rate proportional to their length, our model predicts that the

initial rate of growth is the same as the rate at which subunits enter at the base (9).

We thank Linda Turner and Yuhai Tu for their comments on the manuscript.

This work was supported by the National Institutes of Health (AI016478) and the Rowland Institute at Harvard.

## REFERENCES

1. Chevance, F. F. V., and K. T. Hughes. 2008. Coordinating assembly of a bacterial macromolecular machine. *Nat. Rev. Microbiol.* 6:455–465.
2. Macnab, R. M. 2003. How bacteria assemble flagella. *Annu. Rev. Microbiol.* 57:77–100.
3. Minamino, T., and K. Namba. 2008. Distinct roles of the FliI ATPase and proton motive force in bacterial flagellar protein export. *Nature.* 451:485–488.
4. Paul, K., M. Erhardt, ..., K. T. Hughes. 2008. Energy source of flagellar type III secretion. *Nature.* 451:489–492.
5. Yonekura, K., S. Maki-Yonekura, and K. Namba. 2003. Complete atomic model of the bacterial flagellar filament by electron cryomicroscopy. *Nature.* 424:643–650.
6. Yonekura, K., S. Maki, ..., K. Namba. 2000. The bacterial flagellar cap as the rotary promoter of flagellin self-assembly. *Science.* 290:2148–2152.
7. Homma, M., H. Fujita, ..., T. Iino. 1984. Excretion of unassembled flagellin by *Salmonella typhimurium* mutants deficient in hook-associated proteins. *J. Bacteriol.* 159:1056–1059.
8. Homma, M., and T. Iino. 1985. Excretion of unassembled hook-associated proteins by *Salmonella typhimurium*. *J. Bacteriol.* 164:1370–1372.
9. Turner, L., A. S. Stern, and H. C. Berg. 2012. Growth of flagellar filaments of *Escherichia coli* is independent of filament length. *J. Bacteriol.* 194:2437–2442.
10. Lutz, C., M. Kollmann, ..., C. Bechinger. 2004. Diffusion of colloids in one-dimensional light channels. *J. Phys. Condens. Matter.* 16:S4075–S4083.
11. Berg, H. C. 1993. *Random Walks in Biology*. Princeton University Press, Princeton, NJ.
12. Hasegawa, K., I. Yamashita, and K. Namba. 1998. Quasi- and nonequivalence in the structure of bacterial flagellar filament. *Biophys. J.* 74:569–575.
13. Tanner, D. E., W. Ma, ..., K. Schulten. 2011. Theoretical and computational investigation of flagellin translocation and bacterial flagellum growth. *Biophys. J.* 100:2548–2556.
14. Levy, E. M. 1974. Flagellar elongation as a moving boundary problem. *Bull. Math. Biol.* 36:265–273.